

Title**A Variable and Compact MPFA for Transmissibility Upscaling with Guaranteed Monotonicity.****Abstract**

We propose a new single phase local transmissibility upscaling method that uses spatially varying and compact multi-point flux approximations (MPFA). For each cell face in the coarse upscaled grid, we create a local fine grid region surrounding the face on which we solve two generic local flow problems. The multi-point stencils used to calculate the fluxes across coarse grid cell faces involve the six neighboring pressure values. They are required to honor the two generic flow problems as closely as possible while maximizing compactness and ensuring that the flux approximation is as close as possible to being two-point. The resulting MPFA stencil is spatially varying and reduces to two-point expressions in cases without full-tensor anisotropy. Numerical tests show that the method significantly improves upscaling accuracy as compared to commonly used local methods and also compares favorably with a local-global upscaling method. We constructed a corrector method that adapts the stencils locally to guarantee that the resulting pressure matrix is an M-matrix. This corrector method is needed primarily for cases where strong permeability contrasts are mis-aligned with the grid locally. The corrector method does not affect the flow accuracy. The method is shown to work well for high aspect ratio grids also.

1. Introduction

Subsurface formations may exhibit geometrically complex features with complicated large scale connectivity. They must be included in simulations of flow and transport because they can fundamentally impact simulation results. To reduce computational costs, simulations are generally performed on grids that are coarse compared to the given geocellular grids. These coarsened flow models should adequately represent these key behaviors.

In this work we are concerned with transmissibility upscaling for subsurface formations with complex heterogeneity. Transmissibility upscaling involves finding representative coefficients that relate fluxes at faces between coarse cells to pressures of cells neighboring the faces. Designing a transmissibility upscaling method that is both accurate and computationally efficient is challenging. Local upscaling methods for two-point flux approximations (TPFA), where the flux is computed using pressure value information from the two cells that share the face, are attractive because of their simplicity and ease of implementation. Yet, such methods may not give sufficiently accurate upscaling results in formations with large scale connective paths that introduce full-tensor anisotropy at coarse scales (Gerritsen and Lambers 2006, Chen et al. 2006). Local-global (LG) upscaling, a relatively new upscaling strategy, offers improved accuracy (Chen et al. 2003). Combined with local grid adaptation strategies, LG helps to reduce process dependency (Gerritsen and Lambers 2006). In the presence of full-tensor effects, MPFA methods, which involve additional cells, are desirable. However, MPFA methods add computational costs and may suffer from non-monotonicity (Nordbotten, et al. 2006).

Our goal is to construct a local multi-point flux approximation that accommodates full-tensor anisotropy and guarantees a monotone pressure solution. To achieve this we allow the MPFA stencil to vary spatially, we minimize the number of points involved in the stencil, and we let the stencil revert to a TPFA stencil wherever the accuracy obtained with TPFA is sufficiently high. We name our method the Variable Compact Multi-Point method, or VCMP for short. We exploit the added freedom in allowing the stencils to vary from grid cell to grid cell in order to guarantee monotonicity.

Our current implementation of VCMP is in two spatial dimensions on Cartesian grids with cell-centered finite volume discretizations. The grids may have adaptive grid interfaces. We are extending the method to corner point grids and three-dimensional problems. We limit ourselves here to single phase upscaling methods, but these transmissibilities can also be used for multi-phase simulations.

The VCMP method was first introduced in Lambers, et al. (2006). The general design of the VCMP methods is summarized in section 2. The focus in this paper is on the monotonicity requirement. Our method of enforcing this, which we labeled the M-fix, is described in section 3. Section 4 gives results for a suite of test problems. We discuss the results and future directions in section 5 and list our main conclusions in section 6.

2. Variable Compact Multi-Point (VCMP) methods

2.1. Fine and coarse grid equations

The upscaling strategy is based on single phase, steady and incompressible flow in a heterogeneous reservoir. The governing dimensionless pressure equation is

$$\nabla \cdot (k \cdot \nabla p) = 0. \quad (2.1)$$

Here p is the pressure and k the permeability tensor, all of which are non-dimensionalized by appropriate reference values. We ignored any sources or sinks in the domain. This equation is valid on the fine scale, at which we assume that the permeability tensor as given by geostatistical methods is diagonal, constant in each grid cell and may be highly variable in space. It is common practice to keep the same equation as Eqn. (2.1) for the coarse pressure, with the permeability tensor replaced by the coarse scale effective permeability tensor k^* and p by the coarse scale pressure. This has been found to lead to adequate coarse scale pressure solutions (Durlofsky 1991, Pickup et al. 1994, Bourgeat 1984). In the remainder of the paper we will use Eqn. (2.1) indiscriminately of scale.

2.2. The main ideas behind VCMP

We aim to construct a multi-point finite-volume scheme that has five desirable properties:

- The scheme is "close" to a two-point scheme. Reasons are simplicity, efficiency (maximize matrix sparsity) and consistency (the scheme should reduce to a two-point scheme in the case of homogeneous permeability on a Cartesian grid).
- The scheme is applicable to adaptive grid strategies, such as the CCAR strategy developed in Nilsson, et al. (2005). Adaptivity is an effective way to reduce upscaling errors, and improve representation of connected flow paths in highly heterogeneous formations (Gerritsen and Lambers 2006). This is true especially when combined with a multi-point flux approximation.
- The scheme is very accurate for smooth pressure fields. If the pressure field is not smooth, improved accuracy can be achieved by local grid refinement.
- The scheme performs well for grids with a high aspect ratios, such as are commonly used in reservoir simulators.
- The scheme results in an M-matrix. The M-matrix property ensures monotonicity of the pressure solution, and also is desirable for solver efficiency (Stuben 1983).

The M-matrix property is a sufficient condition to obtain a monotone pressure solution, but not a necessary condition. There exist finite-volume schemes with fixed stencils that achieve monotonicity for a large class of problems but satisfy the M-matrix criterion for only a few cases (Aavatsmark 1996). Although this might suggest that requiring an M-matrix is too restrictive to achieve good accuracy for problems with significant full-tensor effects, our experience is that the M-matrix criterion does not limit the accuracy of our finite-volume scheme, when the flux stencil is spatially variable. This observation is consistent with the findings of (Nordbotten 2006).

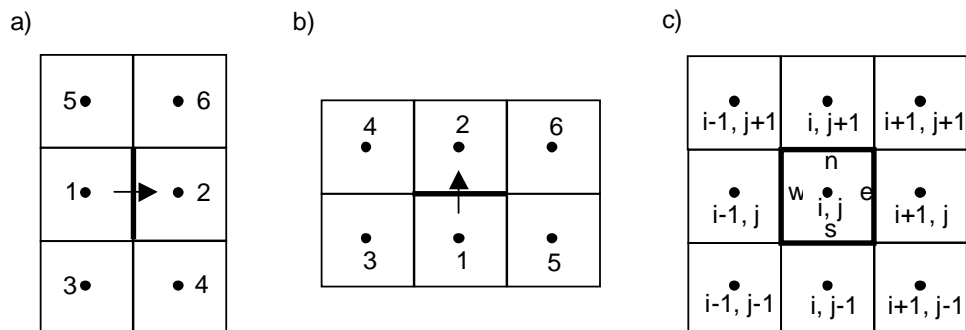


Figure 1: Enumeration of cells is shown for an x-oriented face in (a) and a y-oriented face in (b). The cells potentially included in the stencil for cell (i, j) are shown in (c) along with labels for the four faces defining the cell.

2.3. Construction of VCMP for Cartesian Grids

To create a multi-point flux approximation with the five properties listed above, we allow the MPFA stencil to vary per cell face. Figures 1a and 1b depict an interior face in a Cartesian grid. Our MPFA uses a subset of the six pressure values p_j , $j = 1, \dots, 6$ indicated in the figure. For each j , we let t_j denote the weight that will be assigned to point j in the flux approximation, which has the general form

$$f = -\mathbf{t}^T \mathbf{p},$$

where

$$\mathbf{t} = [t_1 \dots t_6]^T, \quad \mathbf{p} = [p_1 \dots p_6]^T.$$

We solve the pressure equation on the local region of the fine grid containing the six points with two generic Dirichlet boundary conditions. We let $\mathbf{p}^1(x,y)$ and $\mathbf{p}^2(x,y)$ be the solutions of these local problems, and p_j^i denote the value of $\mathbf{p}^i(x,y)$ at point j . For both flow problems pressure varies linearly along the boundary of the local region. The pressure field \mathbf{p}^1 is computed using boundary values chosen so that the pressure gradient is across the face, and \mathbf{p}^2 is obtained from boundary values chosen so that the pressure gradient is parallel to the face.

For $i = 1, 2$, we let f_i denote the coarse-scale flux (sum of fine-scale fluxes) across the face obtained from the local solution $\mathbf{p}^i(x,y)$. To compute the weights t_j , we solve the general optimization problem

$$\min_{\mathbf{t}} \sum_{i=1}^2 \alpha_i^2 |\mathbf{t}^T \mathbf{p}^i - f_i|^2 + \sum_{j=3}^6 \beta_j^2 t_j^2, \quad (2.2)$$

subject to the essential linear constraints

$$\sum_{j=1}^6 t_j = 0, \quad t_{2j-1} \leq 0, \quad t_{2j} \geq 0, \quad j = 1, 2, 3. \quad (2.3)$$

In the current implementation, the weights α_i are chosen to be $|f_i|$ and the weights β_j are chosen to be equal to $(|f_1| + |f_2|)/M$, where M is a tuning parameter. The larger the value of M , the more closely the flows are honored. For small M , we will obtain a two-point flux with $t_j = 0$ for $j = 3, 4, 5, 6$. In this paper, we use $M = 1000$. We solve this problem using the `lsqlin` function from MATLAB's Optimization Toolbox. If any of the weights are found to be negligibly small, we solve the minimization problem again, with the corresponding variables excluded from consideration. Extension to Cartesian Cell-based Anisotropically Refined (CCAR) grids is discussed in Lambers, et al. (2006).

Eqn. (1.1) can be discretized over each cell using

$$0 = f^e - f^w + f^n - f^s = \sum_{k=i-1}^{i+1} \sum_{l=j-1}^{j+1} a_{k,l}$$

where the positions of the fluxes are indicated in Figure 1c. The coefficients $a_{k,l}$ are given by

$$\begin{aligned}
 a_{i-1,j} &= -t_1^w + t_3^n - t_4^s, & a_{i-1,j-1} &= -t_3^w - t_3^s \leq 0, \\
 a_{i+1,j} &= t_2^e + t_5^n - t_6^s, & a_{i-1,j+1} &= -t_5^w + t_4^n \leq 0, \\
 a_{i,j-1} &= -t_1^s + t_3^e - t_4^w, & a_{i+1,j-1} &= t_4^e - t_5^s \leq 0, \\
 a_{i,j+1} &= t_2^n + t_5^e - t_6^w, & a_{i+1,j+1} &= t_6^e + t_6^n \leq 0, \\
 a_{i,j} &= t_1^e - t_2^w + t_1^n - t_2^s > 0.
 \end{aligned}$$

Although this discretization appears to yield a full nine-point stencil, due to the inequality constraints placed on the transmissibilities, generally one or more of the coefficients $a_{i-1,j-1}$, $a_{i-1,j+1}$, $a_{i+1,j-1}$, and $a_{i+1,j+1}$ will be equal to zero. After applying appropriate boundary conditions, the coefficients can be assembled into a linear system $A\mathbf{p} = \mathbf{b}$, where the matrix A has a maximum of nine nonzero entries per row and the nonzero entries in the forcing vector \mathbf{b} arise due to inhomogeneous boundary conditions.

3. The M-fix: Using VCMP's flexibility to guarantee monotonicity

Each entry a_{kl} of A , where $k \neq l$, can be interpreted as the net flux from cell l to cell k when a unit source is placed in cell l . For A to be an M-matrix, we must have $a_{kl} \leq 0$; i.e. a unit source in cell l causes a net flux into cell k . Matrix entries corresponding to diagonal neighbors of each cell are already guaranteed to be negative, thanks to the sign constraints imposed on the weights. To obtain an M-matrix, we therefore have the additional constraint that matrix entries corresponding to direct neighbors are negative.

As these entries are combinations of weights corresponding to several flux approximations, it is not possible to translate this extra requirement into direct constraints on the weights taken together with (2.3). As a result, VCMP does not, in general, produce an M-matrix, although it comes reasonably close in practice, with 10-15% of the off-diagonal elements being positive in the average case, and typically of smaller magnitude than negative elements. To guarantee monotonicity, the constraints on the signs of the elements of A must be enforced in a separate iteration on the fluxes that contribute to the creation of "bad elements" of A in a predictor-corrector type fashion. We call this separate iteration the "M-fix".

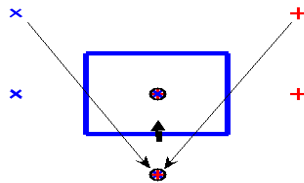


Figure 2. Scenario in which VCMP does not generate an M-matrix. The matrix element corresponding to the bottom center point has the wrong sign. The thin black arrows indicate preferential flow paths. The blue x's, red +'s, and black circles denote cell centers used in the flux approximations for the west, east and south faces, respectively.

Figure 2 illustrates a typical situation in which VCMP fails to produce an M-matrix. Here, preferential flow is from the upper left, to the bottom center, and then to the upper right. The matrix entry corresponding to the bottom neighbor of the center cell has the wrong sign because the correctly-signed contribution from the flux across the

bottom face (t_1^s) is dominated by the contributions from the flux across the left and right faces (t_4^w and t_3^e), which have the incorrect sign. The net flow across the bottom face is relatively small, due to the near-cancellation of the stronger fluxes caused by their opposite orientations. This causes the negative contribution from t_1^s to be too small, relative to the other two positive contributions.

Now, consider the entry a_{kl} of A that corresponds to the direct neighbors cells k and l , where cell k is the center cell in Figure 2. This entry contains contributions from the interaction regions corresponding to the south (s), east (e) and west (w) faces of cell k . Specifically, we have

$$a_{k,l} = t_1^s + t_3^e - t_4^w.$$

The constraints ensure us that $t_1^s \leq 0$, $t_3^e \geq 0$ and $t_4^w \leq 0$. In order for a_{kl} to be negative, it is sufficient to also require that $|t_3^e| \leq |t_1^s|/2$ and $|t_4^w| \leq |t_1^s|/2$.

In general, each entry a_{kl} of A has the form

$$a_{kl} = \sum_{j=1}^{m_{kl}^+} t_{j,kl}^+ + \sum_{j=1}^{m_{kl}^-} t_{j,kl}^-,$$

where each $t_{j,kl}^+ \geq 0$ and each $t_{j,kl}^- \leq 0$. Let \tilde{a}_{kl} be the (k,l) entry of the updated matrix \tilde{A} . To ensure that \tilde{A} is an M-matrix, we impose the additional constraints

$$\left| \tilde{t}_{j,kl}^- \right| \geq \left| \tilde{t}_{j,kl}^+ \right| \quad \text{and} \quad \tilde{t}_{j,kl}^+ \leq \frac{1}{m_{kl}^+} \left(\sum_{j=1}^{m_{kl}^+} \left| \tilde{t}_{j,kl}^- \right| \right) \quad (3.1)$$

on the nonnegative and nonpositive contributions to \tilde{a}_{kl} , and recompute each flux whose weights contribute to \tilde{a}_{kl} . The result is an M-matrix \tilde{A} , provided all of the optimization problems for the multi-point flux approximations can be solved, which is the case in practice. Because greater weight is imposed on the flow criterion in (2.2) the M-matrix is obtained without affecting flow accuracy much.

For a CCAR grid, an alternative to the M-fix is adaptation of the grid by refinement of faces corresponding to incorrectly signed entries (such as the bottom face in Figure 2). The result is a sequence of successively finer grids that converges to a grid that yields an M-matrix with the original VCMP algorithm.

It is important to note that it is the flexibility of VCMP that makes the M-fix possible. VCMP admits any flux approximation that satisfies the previously stated constraints, preferring those that are also close to a two-point flux and honor local flow. The M-fix merely tightens these constraints, which are still easily satisfied in practice.

4. Numerical results

4.1. The test suite

Our test suite consists of three types of fine permeability fields that are used in the experiments described in this section. All have dimension $L_x \times L_y$, where $L_x = 256$ and $L_y = 64$. The fields are:

- A realization with medium correlation lengths of $l_x = 15$, $l_y = 5$, aligned with the grid
- A realization with long correlation lengths of $l_x = 75$, $l_y = 5$, not aligned with the grid
- A channelized domain, based on layer 44 from the SPE 10 Comparative Project (Christie and Blunt 2001)

All fine grids are of size 256×64 , with $\Delta x = \Delta y = 1$. For all cases generated using 2-point statistics, we use mean 3.0 and standard deviation 1.735, which corresponds to a log-normal distribution.

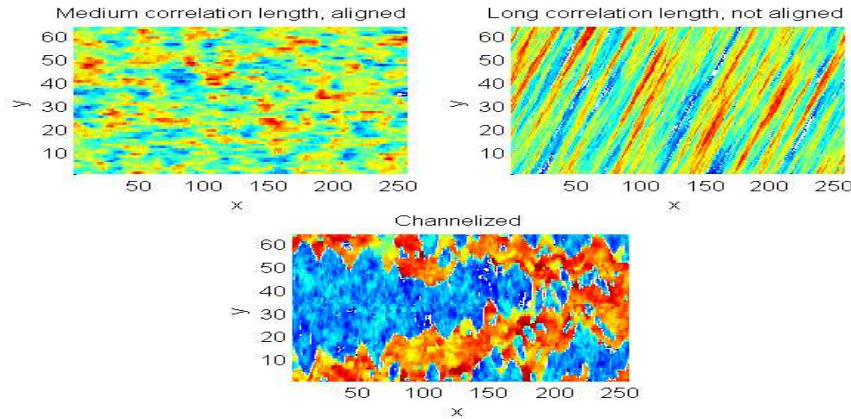


Figure 3. Fine-scale permeability fields in the test suite. Top left: medium correlation length, aligned to grid. Top right: long correlation length, not aligned to grid. Bottom: channelized domain.

4.2. VCMP without monotonicity fix

Table 4.1 lists percentage errors in total flow for various boundary conditions and upscaling methods, including VCMP, on the permeability fields with high correlation length, not aligned to the grid, and with channels. For these cases, VCMP is used in conjunction with extended local regions of the same size as those used in the other upscaling methods. We see that in both cases, VCMP is clearly the most robust, and is also the most accurate in most cases, see also Lambers et al. (2006).

Flow	Long corr. Length, not aligned to grid				Channelized			
	Fine scale flow	EL	LG	VCMP	Fine scale flow	EL	MLLG	VCMP
y-direction	97.11	18.31	3.60	2.18	35.77	10.42	0.40	2.23
lower left	55.85	36.67	9.16	0.44	7.41	15.18	0.90	2.55
upper right	-58.36	30.14	0.92	1.27	-28.07	8.84	1.12	0.59
p=x+y	-16132.22	38.90	3.96	0.92	-16696.89	62.65	28.34	4.55

Table 4.1: Flow results for (1) the permeability field with high correlation length, not aligned to the grid, and (2) channels, both shown in Figure 3. The table lists percentage error in total flow for various boundary conditions, and for various upscaling methods: extended local (EL), local-global (LG, or MLLG in the CCAR case), and VCMP with extended local regions (VCMP-EL). For the case with long correlation length, the coarse grid is a 32x16 uniform grid. For the channelized case, the coarse grid is a CCAR grid with no more than 398 cells.

4.3. VCMP with monotonicity fix (M-fix)

Table 4.2 lists percentage errors in total flow for the permeability fields with long correlation length, not aligned to the grid, and with channels. We see that for both permeability fields and nearly all boundary conditions, little accuracy is sacrificed in exchange for obtaining an M-matrix.

Flow	Long corr. Length, not aligned to grid			Channelized		
	Fine scale	Without M-fix	With M-fix	Fine scale	Without M-fix	With M-fix
In y-direction	97.11	2.18	4.29	35.77	2.23	2.80
From lower left	55.85	0.44	0.55	7.41	2.55	2.21
From upper right	-58.36	1.27	0.43	-28.07	0.59	0.85
p=x+y	-16132.22	0.92	4.04	-16696.89	4.55	3.98

Table 4.2: Flow results for the permeability fields with (1) high correlation length, not aligned to the grid, and (2) channels, both shown in Figure 3. The table lists percentage error in total flow for various boundary conditions, and for VCMP with extended local regions (VCMP-EL), both with and without the M-fix. For the case with long correlation length, the coarse grid is a 32x16 uniform grid. For the channelized case, the coarse grid is a CCAR grid with no more than 398 cells.

4.4. VCMP with M-fix on high aspect ratio grids

Finally, we examine the accuracy of VCMP, with the M-fix, on grids with high aspect ratios. Table 4.3 lists percentage errors in total flow for the permeability field with medium correlation length, aligned to the grid. In all cases, the extended region used for each local solve is sized so that it has a 2:1 aspect ratio. Furthermore, VCMP is modified so that it uses constant-pressure/no-flow boundary conditions for local solves, instead of Dirichlet boundary conditions as described in Lambers et al. (2006). We see that although there is deterioration in the accuracy as the aspect ratio increases, the accuracy is still quite reasonable even for the 16:1 case. Future work will include further investigation of grids with high aspect ratios.

Flow	Fine scale	EL, 2:1	VCMP, 2:1	EL, 8:1	VCMP, 8:1	EL, 16:1	VCMP, 16:1
In y-direction	45.46	0.67	0.66	0.34	0.75	0.68	0.45
From lower left	14.91	1.93	1.80	1.76	3.69	3.55	6.19
From upper right	-19.60	0.02	0.11	1.93	1.39	7.30	8.38
$p=x+y$	-5909.33	0.76	0.06	0.66	1.80	2.80	8.26

Table 4.3: Flow results for the permeability field with medium correlation length, not aligned to the grid, shown in Figure x. The table lists percentage error in total flow for various boundary conditions, various aspect ratios, using extended local (EL), and VCMP with extended local regions (VCMP-EL) and the M-fix. For the 2:1 and 8:1 cases, the coarse grid is a 512-cell Cartesian grid. For the 16:1 case, the coarse grid is a 256-cell Cartesian grid.

5. Discussion

Results of the previous section, and additional results presented in Lambers, et al. (2006) suggest that VCMP has the best overall performance for our suite of test problems, and is a very promising approach.

The VCMP method described in section 2 does not strictly guarantee that the pressure matrix will be an M-matrix. Monotonicity problems occur mostly in cases where the permeability is strongly misaligned with the grid and the permeability contrasts are high. However, the M-fix proposed in this paper corrects the matrix and restores monotonicity. Most importantly, we show in this study that the M-fix does not lower the flow accuracy. The M-fix is made possible by the flexibility provided by the VCMP method in choosing the transmissibility coefficients.

VCMP and the M-fix have a straightforward extensions to Cartesian and CCAR grids in three dimensions that involve three local flow problems for each coarse face. In 3D, the VCMP stencil will contain between 7 and 19 point whereas a full multipoint stencil contains 27 points. The extensions of VCMP to non-orthogonal grids or unstructured grids are possible as discussed in Lambers, et al. (2006).

6. Summary and Conclusions

We have introduced a new (extended) local transmissibility upscaling scheme that we are calling the variable compact multi-point method or simply VCMP. VCMP accommodates full-tensor anisotropy which is generally present in coarse scale flow problems. The stencil adapts to the orientation of the underlying fine permeability distribution. In addition to accurately predicting global flow rates, upscaled transmissibility fields computed with VCMP locally agree well with averaged fine scale results.

Lack of monotonicity may occur in cases where strong permeability contrasts are not aligned with the grid. The proposed M-fix can be used as a corrector step in the VCMP method to guarantee the pressure matrix is an M-matrix. For the wide range of test cases presented in this paper, the M-fix does not affect flow accuracy. We have shown that VCMP with the M-fix also works well for the case of high aspect ratio grids that generally pose challenges for MPFA methods.

References

- Aavatsmark, I., Barkve, T., and Mannseth, T. [1996] Discretization on Non-Orthogonal, Quadrilateral Grids for Inhomogeneous, Anisotropic Media. *Journal of Computational Physics* 127, 2-14.
- Bourgeat, A. [1984] Homogenized Behavior of Two-Phase Flows in Naturally Fractured Reservoirs with Uniform Fractures Distribution. *Computational Methods in Applied Mechanics and Engineering* 47, 205-216.
- Chen, Y., Durlofsky, L.J., Gerritsen, M.G., and Wen, X.H. [2003] A coupled local-global upscaling approach for simulating flow in highly heterogeneous formations. *Advances in Water Resources* 26, 1041-1060.
- Chen, Y., Mallison, B.T., and Durlofsky, L.J. [2006] Nonlinear Two-point Flux Approximation for Modeling Full-tensor Effects in Subsurface Flow Simulations. *Computational Geosciences*, submitted.
- Christie, M.A., and Blunt, M.J. [2001] Tenth SPE comparative solution project: a comparison of upscaling techniques. *SPE Reservoir Evaluation Eng* 4, 308-17.
- Durlofsky, L.J. [1991] Numerical Calculation of Equivalent Grid Block Permeability Tensors for Heterogeneous Porous Media. *Water Resources Research* 27, 699-708.
- Gerritsen, M.G., and Lambers, J.V. [2006] A Specialized Upscaling Method For Adaptive Grids: Tight Integration of Local-Global Upscaling and Adaptivity Leads to Accurate Solution of Flow in Heterogeneous Formations. *Computational Geosciences*, submitted.
- Lambers, J.V., Gerritsen, M.G., and Mallison, B.T. [2006] Accurate Local Upscaling with Variable Compact Multi-point Transmissibility Calculations. *Computational Geosciences*, submitted.
- Nilsson, J., Gerritsen, M.G., and Younis, R.M. [2005] A Novel Adaptive Anisotropic Grid Framework for Efficient Reservoir Simulation. *Proc. of the SPE Reservoir Simulation Symposium*, SPE 93243.
- Nordbotten, J.M., Aavatsmark, I., and Eigestad, G.T. [2006] Monotonicity of Control Volume Methods. *Numerische Mathematik*, submitted.
- Pickup, G.E., Ringrose, P.S., Jensen, J.L., and Sorbie, K.S. [1994] Permeability Tensors for Sedimentary Structures. *Mathematical Geology* 26, 227-250.
- Stuben, K. [1983] Algebraic Multigrid (AMG): experiences and comparisons. *Appl. Mathematics and Computation* 13, 419-452.